International Journal of Greenhouse Gas Control 90 (2019) 102791

Contents lists available at ScienceDirect

International Journal of Greenhouse Gas Control

journal homepage: www.elsevier.com/locate/ijggc

An advancement in CO_2 utilization through novel gas switching dry reforming

Ambrose Ugwu[a,*], Abdelghafour Zaabout[b], Shahriar Amini[a,b,*]

[a] Norwegian University of Science and Technology (NTNU), Trondheim, Norway
[b] Process Technology department, SINTEF Industry, Trondheim, Norway

ARTICLE INFO

Keywords:
Chemical looping
Dry reforming
CO_2 capture and utilization
Gas switching technology
Hydrogen and syngas production
Natural gas reforming.

ABSTRACT

This study is the first experimental demonstration of CO_2 capture and utilization for dry methane reforming using a novel chemical looping concept, "Gas Switching Dry Reforming" (GSDR) to produce syngas. The new reactor concept utilizes a single fluidized bed reactor to complete redox (reactions) cycles by alternating air and gaseous fuel feeds, generating heat and near pure CO_2 for usage in a consecutive dry reforming stage. Autothermal operation of GSDR was achieved using NiO/Al_2O_3 oxygen carrier, in a three-stage configuration where pure CO is used in the reduction stage while CH_4 and CO_2 are fed simultaneously in the reforming stage. Most of the heat duties of the process is generated by the exothermic oxidation reaction. The reforming stage is very sensitive to temperature with very good CH_4 and CO_2 conversion achieved at 850 °C but dropped rapidly at lower temperatures. Carbon deposition is a major issue affecting the performance of GSDR process although this is found to be minimized by a combination of high operating temperature and larger CO_2/CH_4 ratio, but also led to low H_2/CO molar ratio driven by the reversed water gas shift reaction. Reducing the utilization of the oxygen carrier by 50% also proves to decrease carbon deposition by 62% due to the presence of latent oxygen on the oxygen carrier. However, CH_4 and CO_2 conversion are affected negatively resulting in a drop of ~22%. An excellent opportunity for maximizing the energy efficiency of the GSDR is by integration with a Gas-To-Liquid (GTL) Fisher Tropsch to use outlet gas stream from the reforming as feedstock to GTL while the unconverted hot gasses from GTL process is fed to the reduction stage of GSDR.

1. Introduction

CO_2 and CH_4 are the two major primary greenhouse gases (GHG) that pose a threat to the world today through global warming and climate change. As global energy demand and consumption of fossil fuel continue to increase, CCS remains a viable and cost-effective technology to combat greenhouse gas emission and achieve the Paris Climate Accord goals of maintaining the global temperature increase within 1.5 °C (IPCC, 2018). With the projection that natural gas would be the fastest growing fossil fuel in the coming decades (Nejat et al., 2015; Baltagi et al., 2002), CO_2 methane reforming (dry reforming) would therefore be an attractive technology that can sustainably utilize CO_2 and the abundant natural gas (CH_4) not only to reduce GHG emission but also produce valuable products (syngas) for various applications (Muraza and Galadima, 2015a; Sternberg et al., 2017; Ewbank et al., 2014).

The particularity of syngas produced from the dry reforming process is the H_2/CO molar ratio which is close to unity (*Reaction* ***1***), being especially suitable for the synthesis of liquid hydrocarbons, (through the Fisher Tropsch process), oxygenates and other industrially relevant chemicals (Usman et al., 2015a). Although the working principle of dry reforming has been experimentally tested, where tens of studies were published for this process mainly about catalyst development (Wei and Iglesia, 2004a, b; Wei and Iglesia, 2004c, d; Wei and Iglesia, 2004e, f), there are various factors that are still limiting its industrial deployment. Firstly, the reaction is highly endothermic making the process energy intensive requiring an operating temperature above 800 °C in order to achieve high conversion (Aramouni et al., 2017). This involves large CO_2 emissions as fossil fuel is used for supplying heat to the endothermic dry reforming reactions. Another major drawback that hampers the commercialization of the process is the high degree of carbon deposition through different mechanisms (*Reaction* ***3*** and *Reaction* ***4***), leading to fast catalyst deactivation (Oyama et al., 2012). Several studies attempted to tackle the carbon deposition issue through catalyst development (Hou et al., 2006; Carrara et al., 2008; Chen et al., 1998). Alternatively, it has been shown that a CO_2/CH_4 molar ratio

* Corresponding authors at: Norwegian University of Science and Technology (NTNU), Trondheim, Norway.
E-mail addresses: ambrose.ugwu@ntnu.no (A. Ugwu), shahriar.amini@sintef.no (S. Amini).

https://doi.org/10.1016/j.ijggc.2019.102791
Received 8 March 2019; Received in revised form 24 June 2019; Accepted 15 July 2019
Available online 26 July 2019

Nomenclature

Abbreviations

CCS	Carbon capture and storage
CLDR	Chemical Looping Dry Reforming
CLR	Chemical Looping Reforming
GSDR	Gas Switching Dry Reforming
GSR	Gas Switching Reforming
GST	Gas Switching Technology
GTL	Gas-To-Liquid
RWGS	Reverse Water Gas Shift

Symbols

C_{dep}	Carbon deposition
D_{10}	Diameter of the catalyst which 10% of a sample mass is smaller than
D_{50}	Diameter of the catalyst which 50% of a sample mass is smaller than
D_{90}	Diameter of the catalyst which 90% of a sample mass is smaller than
n_{C,out_ref}	Mole of C at the gas outlet during reforming stage
n_{CH_4,in_ref}	Mole of CH_4 fed during reforming stage
n_{CH4,out_ref}	Mole of CH_4 at the gas outlet during reforming stage
n_{CO,out_oxi}	Mole of CO at the gas outlet during oxidation stage
n_{CO_2,out_oxi}	Mole of CO_2 at the gas outlet during oxidation stage
n_{CO,out_red}	Mole of CO at the gas outlet during reduction stage
n_{CO,in_red}	Mole of CO fed during reduction stage
n_{CO,out_ref}	Mole of CO at the gas outlet during reforming stage
n_{CO_2,in_ref}	Mole of CO_2 fed during reforming stage
n_{CO_2,out_ref}	Mole of CO_2 at the gas outlet during reforming stage
n_{H_2,out_ref}	Mole of H_2 at the gas outlet during reforming stage
n_{H_2O,out_ref}	Mole of H_2O at the gas outlet during reforming stage
s_{CO}	CO selectivity
s_{H2}	H_2 selectivity
$\varnothing_{syngas}$	Overall syngas selectivity
γ_{CH_4}	CH_4 conversion
γ_{CO}	CO conversion
γ_{CO_2}	CO_2 conversion

higher than stoichiometry (unity) could improve the reaction kinetics and lead to high syngas yield (Aramouni et al., 2017). Consequently, this leads to low syngas purity due to the presence of excess CO_2 in the produced syngas. Another side effect of feeding excess CO_2 is the low H_2 yield resulting from the reverse water-gas shift reaction. It is, therefore, crucial to develop new technologies that can address the aforementioned issues of dry reforming to make the process environmentally and economically viable for commercial deployment.

$$CH_4 + CO_2 \rightarrow 2CO + 2H_2 \ (\Delta H_{298K} = +247KJmol^{-1}) \quad (1)$$

$$CO_2 + H_2 \leftrightarrow CO + H_2O \ (\Delta H_{298K} = +41KJmol^{-1}) \quad (2)$$

$$CH_4 \rightarrow C + 2H_2 \ (\Delta H_{298K} = +74.9KJmol^{-1}) \quad (3)$$

$$2CO \leftrightarrow C + CO_2 \ (\Delta H_{298K} = -172.4KJmol^{-1}) \quad (4)$$

This paper demonstrates a novel chemical looping technology "Gas Switching Dry Reforming (GSDR)" which combines carbon capture and utilization in a single process to produce syngas (H_2 + CO). The aim is to use a novel chemical looping reactor design that can be easily pressurized and scaled up to minimize CO_2 emissions in dry reforming processes by integrating carbon capture in one step and possible utilization of the captured CO_2 as a feedstock for ***Reaction 1*** in another step as explained in Section 1.1. If successfully demonstrated and scaled up, this technology can offer a sustainable solution for the costly CO_2 transport and storage issue hindering the implementation of CCS technology. This paper also explores and maps out the opportunities offered by the proposed technology for minimizing carbon deposition on the catalyst/oxygen carrier and maximizing the fuel conversion.

1.1. Gas switching dry reforming

Chemical looping technology is an emerging low-carbon technology which typically employs an interconnected fluidized bed reactor system that circulates a metal oxide (oxygen carrier) to transfer oxygen from the air reactor to the fuel reactor for combusting fuel gases in a N_2-free environment, producing a pure CO_2 stream ready for storage or further utilization (Fig. 1 -Left) (Ishida et al., 1987; Lyngfelt et al., 2001). The low energy penalty of this technology relative to other CCS technologies has led to the extension to other energy-intensive processes such as steam-iron process, low emission coal conversion, methane reforming, etc. (Anthony, 2008; Rydén and Arjmand, 2012). The major drawback of the traditional chemical looping systems using CFB configuration is the operational challenges associated with high-pressure processes

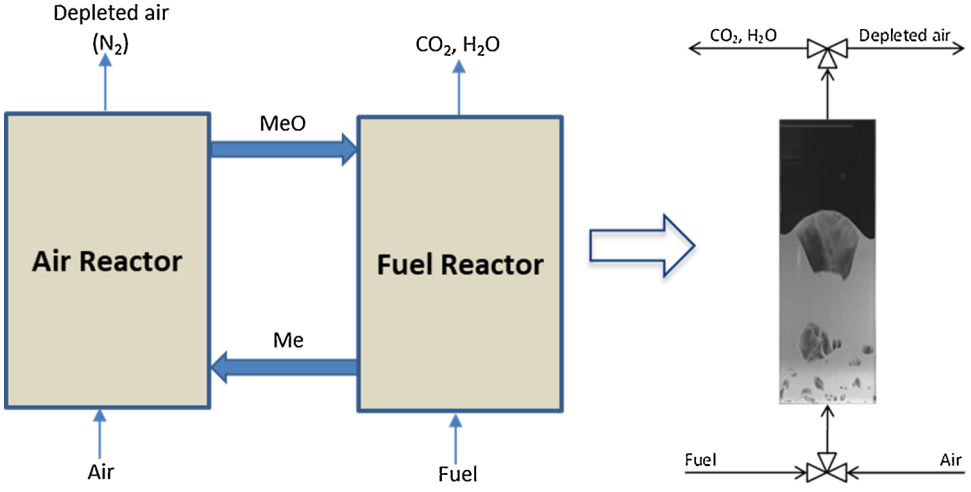

Fig. 1. Left: Conventional Chemical Looping Combustion Reactor Concept. Right: Simplified Gas Switching Reactor Concept for fuel combustion with integrated CO_2 capture.

reflecting why most of the experimental demonstrations were carried out under atmospheric conditions (Proell et al., 2010; Kronberger et al., 2004; Linderholm et al., 2008; Johansson et al., 2006; Ding et al., 2012; Kolbitsch et al., 2010; Ryden and Lyngfelt, 2006; Rydén et al., 2006; de Diego et al., 2009). Solid circulation between interconnected reactors would be difficult to achieve under pressurized conditions given that each reactor is pressurized independently while fulfilling the essential need for heat and mass balance. Any instantaneous pressure imbalance between the reactors would induce instabilities and could result in leakages through the sealing devices, thereby increasing the risk of explosion. Even with these limitations, high-pressure operation is however prerequisite in order to maximize the overall process efficiency.

To address the challenges facing pressurized chemical looping applications, recent research has focused on the development o alternative reactor designs with the ability to operate under pressurized conditions (Hamers et al., 2014; Zaabout et al., 2013a; Noorman et al., 2007; Hamers et al., 2013; Zaabout et al., 2014). One of the promising reactor designs is the Gas Switching Technology (GST) that utilizes only one fluidized bed reactor and avoids solid circulation by alternating the feeds of the oxidizing and reducing gases to depict different redox stages as shown in Fig. 1- right. The reactor choice for a fluidized bed is driven by the previous study that fluidized bed reactors exhibited the highest activity, catalyst stability, lower carbon deposition, and higher conversion compared to a fixed-bed counterpart (Usman et al., 2015b). Since solid circulation is avoided, GST does not require separation systems like cyclone and loop seals making it less expensive and simpler compared with traditional chemical looping systems. The GST reactor concept has been applied for power production through combustion (Zaabout et al., 2013b, 2017; Zaabout et al., 2018) and syngas production through steam methane reforming with integrated CO_2 capture (Wassie et al., 2017a, 2018; Zaabout et al., 2019; Ugwu et al., 2019). Experimental demonstration studies have also proved the ease of autothermal operation for both combustion and reforming (Zaabout et al., 2017; Wassie et al., 2017a, 2018). To capitalize on this success, this study extends the GST concept to dry reforming process for syngas production referred to as Gas Switching Dry Reforming (GSDR).

The working principle of Gas Switching Dry Reforming (GSDR) is very similar to the Gas Switching Reforming (GSR) demonstrated earlier for syngas production with integrated CO_2 capture (Wassie et al., 2017a; Zaabout et al., 2019). It is a three-stage process as illustrated in Fig. 2 comprising of a **fuel stage** where the oxygen carrier is reduced to metallic radical to catalyze the endothermic dry reforming reaction at the consecutive **reforming stage**. The third stage is the **air stage** where the oxygen carrier is reoxidized to generate the heat needed for the highly endothermic dry reforming reaction. In this process, the solid particle plays simultaneous roles of oxygen carrier and catalyst for dry methane reforming. To demonstrate autothermal operation of GSDR process, part of the CO produced during the reforming stage is used as fuel in the reduction stage to sustain the bed temperature since the reduction reaction of NiO with CO is slightly exothermic. The separate reduction stage of GSDR will especially be beneficial if the GSDR is integrated with a Gas-To-Liquid (GTL) process, allowing the unconverted GTL outlet gases to be fed to the reduction stage of GSDR (Fig. 3), thereby maximizing fuel usage and overall process efficiency. However, if similar GSDR process should be implemented with the conventional chemical looping concept using the circulating fluidized bed (CFB) configuration, three interconnected reactors would be required as shown in Fig. 2-left, thus increasing the difficulties in controlling the solids circulation rate to meet the tight heat and mass balance of the three separate reactors. A two-reactor CFB configuration could work if the fuel reactor is fed with methane for simultaneous reduction of oxygen carrier and reforming. In this case, the oxidation degree and circulation rate of the oxygen carrier should be well controlled for maximizing the selectivity to syngas instead of CO_2 (if excess of oxygen is available on the oxygen carrier) while accurately supplying the heat needed for the endothermic dry reforming reaction. The two-reactor CFB configuration would also make it difficult to feed GTL unconverted gasses, thereby reducing the process flexibility and its potential for maximizing its energy efficiency. A major advantage of GSDR process is the efficient use of the reaction heat produced during the oxidation stage for the endothermic reforming stage, since the reactions occur in a single reactor vessel, thus facilitating its autothermal operation (Ortiz et al., 2011). The redox reactions involved when a Ni-based oxygen carrier is used are specified in (***Reaction 5*** and ***Reaction 6***) (Zaabout et al., 2013b, a), while ***Reaction 1*** to ***Reaction 4*** takes place in the reforming stage.

Fuel stage

$$CO + NiO \rightarrow Ni + CO_2 \ (\Delta H_{298K} = -43.3 KJmol^{-1}) \quad (5)$$

Air stage

$$Ni + O_2 \rightarrow 2NiO \ (\Delta H_{298K} = -479.4 KJmol^{-1}) \quad (6)$$

Like other gas switching concepts, GSDR faces the challenge of undesired mixing when switching the inlet feed gases. In the case of GSDR, undesired mixing will cause some N_2 to leak into the syngas and some CO_2 to escape to the atmosphere with the depleted air. This leakage is small for reforming concepts though. For example, reactor modeling in a previous study on GSR showed that 97% CO_2 capture could be achieved despite this undesired mixing (Nazir et al., 2018).

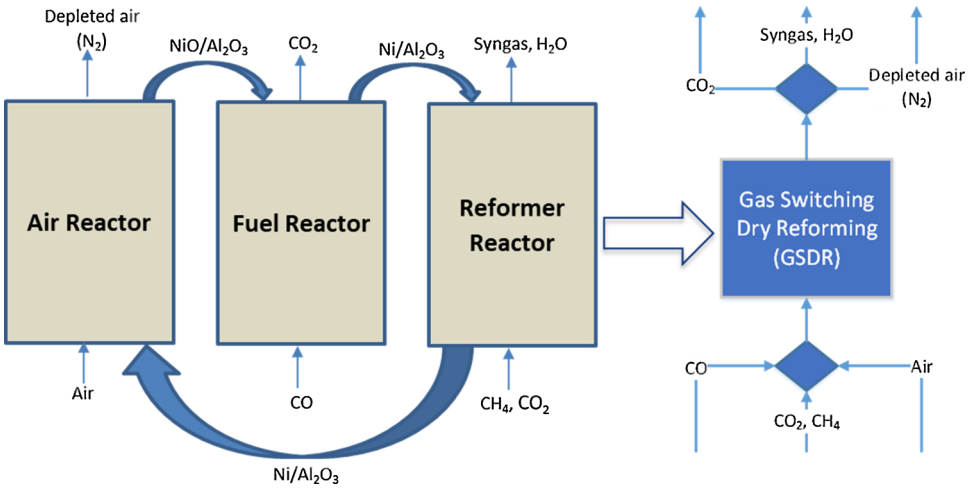

Fig. 2. Conceptual schemes of dry reforming process. Left; Conventional chemical looping route. Right; Gas Switching Dry Reforming(GSDR) route.

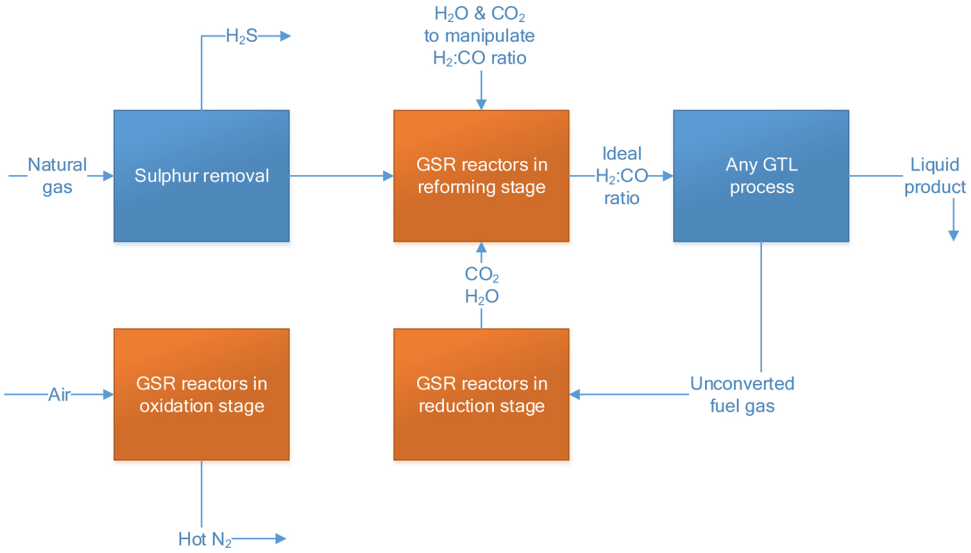

Fig. 3. Possible integration of GSDR with gas-to-liquids (GTL) processes.

2. Experiment and methods

2.1. Experimental setup

The core of the experimental set up used for the demonstration of the GSDR concept consists of a fluidized bed reactor with a cylindrical column (5 cm in inner diameter and 50 cm in height) and a freeboard zone (Fig. 4). The freeboard is an expanding conic zone (from 5 cm in the lower end diameter to 10 cm at the top end) followed by a cylindrical part to minimize particles elutriation. The total height of the reactor, including the body and the freeboard, is 90 cm. The reactor vessel was made of Inconel 600 to withstand high-temperature gas-solids reactive flows (up to 1000 °C). A porous plate with 20 μm mean pore size and 3 mm thickness, made from Inconel 600, was used as a gas distributor placed at the bottom of the reactor. External electrical heating elements wound around the reactor vessel was used to heat up the reactor to a target temperature before starting autothermal GSDR process. A 25 cm thickness insulation was installed, surrounding the reactor, combining blankets and vermiculate. Mass flow controllers from Bronkhorst BV were used for feeding gases to the reactor. A three-

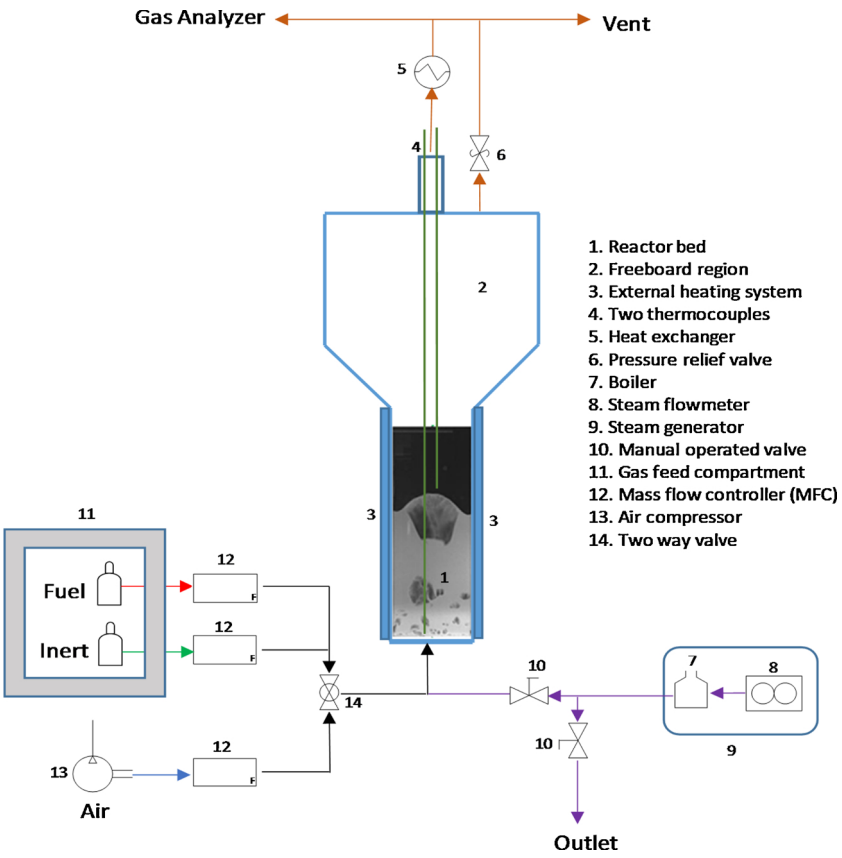

Fig. 4. GSDR Experimental setup.

way electrical valve was used to separate the air and fuel feeds when cycling the process stages. A cooler was installed at the outlet of the reactor to cool down the stream of hot gases before being sent to the vent. The gas composition was measured using an ETG syngas analyzer sampling the gas on the outlet gas stream. The temperature was measured at two positions in the reactor, 2 cm and 20 cm above the gas distributor using two thermocouples inserted through the middle axis of the reactor. All the measurement instruments and flow controlling devices were controlled through a LabVIEW application. The LabVIEW application was also used for data acquisition and logging.

2.2. Methodology

The GSDR was demonstrated using a highly active NiO/Al_2O_3 oxygen carrier manufactured by VITO through spray drying was used for the GSDR demonstration. The total mass of the oxygen carrier used in this study is 623 g corresponding to a 0.3 m static bed height. The oxygen carrier has particle size cut-offs D_{10}, D_{50} and D_{90} of 117.4, 161.7 and 231.3 μm respectively. About 33% weight of active NiO is available for reaction. The powder has a loosely packed density of 1950 kg/m^3 and a tapped density of 2166 kg/m^3. This oxygen carrier used in chemical looping studies including combustion (Zaabout et al., 2013b; Bolhar-Nordenkampf et al., 2009; Cho et al., 2004; Zaabout et al., 2015b) and reforming (Wassie et al., 2018, 2017b) where it has been excellent stability and catalytic activity for reforming.

In the present study, typical GSDR cycles were completed starting with the reduction stage by feeding CO to react with NiO to produce Ni to catalyze the dry reforming reaction. CO is preferred in the reduction stage because of its high reactivity and the slightly exothermic reaction with NiO allowing sustaining high temperature in the reactor before the start of the dry reforming stage. The reduction stage is followed immediately by the reforming stage where the reduced Ni-based oxygen carrier serves as a catalyst for the dry reforming to produce syngas (CO and H_2). The energy demanding reforming stage is followed by an air stage where pure air is fed to oxidize Ni back to NiO while producing the heat required to bring back the process to the same temperature at the start of the cycle.

Experiments were performed under different target operating temperatures from 850 - 750 °C (the temperature at the start of the reduction stage) at atmospheric pressure. The reactor was first heated up using external electric heating element up to the target temperature, followed by the autothermal GSDR experiments while the heaters are turned off. Following the three-stages process (reduction, reforming and oxidation) configuration.12.8 nl/min CO was fed into the reactor for 5 min, 3.2 nl/min CH_4 (and CO_2 at various CH_4/CO_2 ratios) in the reforming stage and 15 nl/min feed of pure air in the oxidation stage. The feed rates used ensured operating the reactor at velocities way beyond the minimal fluidization velocity of the powder.

As mentioned earlier, real-time temperature and pressure measurements were logged using a Labview application while the online gas composition was measured using an ETG Syngas analyzer. The reactor performance at different temperatures was evaluated using the following measures: fuel conversion, CO_2 conversion, CO and H_2 selectivity, degree of carbon deposition, syngas purity. The experimental results were compared with equilibrium predictions.

2.2.1. Reactor performance indicators

The objective of the GSDR process is to convert a hydrocarbon fuel (CH_4 in this study) and CO_2 to syngas (H_2 and CO). Therefore, it is desired to maximize the fuel conversion in the reduction stage and CH_4 and CO_2 conversion in the reforming stage in order to maximize syngas production and CO_2 capture and utilization. The following performance indicators have been defined to evaluate reactor performance.

Firstly, the CO conversion in the reduction stage is quantified as follows:

$$\gamma_{CO} = 1 - \frac{n_{CO,out\_red}}{n_{CO,in\_red}} \tag{7}$$

Syngas ratio is an important parameter that determines the quality and application of the product syngas. This parameter is defined as:

$$\frac{H_2}{CO} = \frac{n_{H_2,out\_ref}}{n_{CO,out\_ref}} \tag{8}$$

The methane conversion in the reforming stage is quantified as follows:

$$\gamma_{CH_4} = 1 - \frac{n_{CH4,out_{ref}}}{n_{CH_4,in_{ref}}} \tag{9}$$

The carbon present in methane converts to solids carbon that deposits on the oxygen carrier and CO. Thus, the selectivity of converted methane to CO is quantified as follows:

$$s_{CO} = \frac{n_{CO,out\_ref}}{n_{CO,out\_ref} + n_{C,out\_ref}} \tag{10}$$

The selectivity of converted methane to H_2 is also quantified as:

$$s_{H2} = \frac{n_{H2,out\_ref}}{2(\gamma_{CH_4} {}^{*} n_{CH_4,in\_ref})} \tag{11}$$

The degree of CO_2 conversion in the reforming stage is:

$$\gamma_{CO_2} = 1 - \frac{n_{CO_2,out_{ref}}}{n_{CO_2,in_{ref}}} \tag{12}$$

Significant carbon deposition also took place during the reforming and fuel stage and this deposited carbon was released in the oxidation

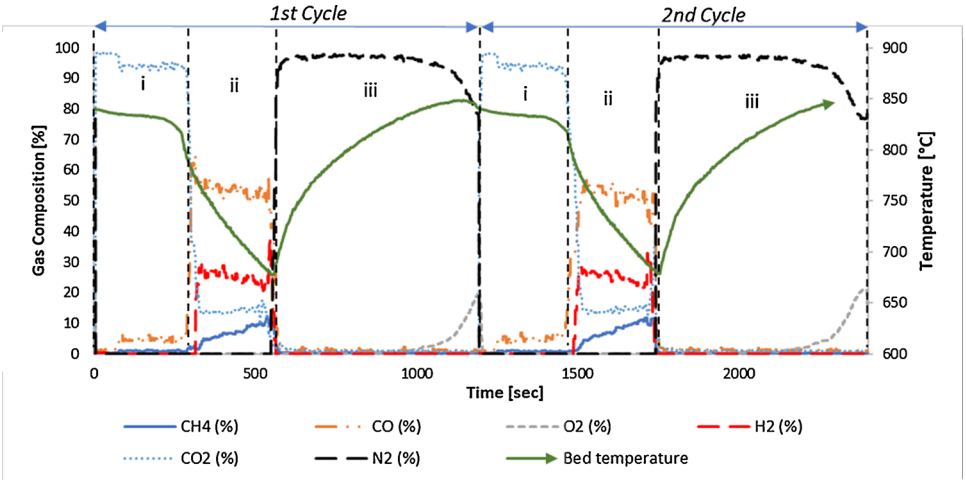

Fig. 5. Two autothermal GSDR cycles showing transient gas composition and temperature profile. The reduction starts at a temperature of 850 °C (target temperature). 1 bar operating pressure, CO_2/CH_4 molar ratio of 2 and gas flowrate as follows: CO- 12.8 nl/min, CH_4-3.2 nl/min, CO_2-6.4 nl/min, Air – 10 nl/min. i, ii and iii represent the reduction, reforming and oxidation stages respectively.

stage. The fraction of carbon deposition is therefore quantified as follows based on the oxidation stage outlet and the total methane entering the fuel stage:

$$C_{dep} = \frac{n_{CO,out\_oxi} + n_{CO_2,out\_oxi}}{\gamma_{CH_4}{}^{*}n_{CH_4,in\_ref} + \gamma_{CO_2}{}^{*}n_{CO_2,in\_ref} + \gamma_{CO}{}^{*}n_{CO,in\_red}} \quad (13)$$

Finally, the overall syngas selectivity produced during the reforming stage is quantified as follows:

$$\varnothing_{syngas} = \frac{n_{CO,out\_ref} + n_{H_2,out\_ref}}{n_{H_2,out\_ref} + n_{CO,in\_ref} + n_{C,out\_ref} + n_{H_2O,out\_ref}} \quad (14)$$

3. Result and discussion

3.1. Demonstration of GSDR concept

In order to achieve autothermal operation, a three-stages GSDR process (reduction, reforming and oxidation) was designed where CO was used in a separate reduction stage due to the slightly exothermic reaction between CO and NiO enabling maintaining a high temperature in the reactor before starting the consecutive reforming stage. Using CO in the reduction stage will also implicitly demonstrate the ability to integrate GSDR with a GTL process as discussed in Section 1.1, where CO is the main component in the GTL off-gasses together with H_2 that was shown to convert well with NiO (Wassie et al., 2017a; Zaabout et al., 2015a). CH_4 and CO_2 (CH_4:CO_2 = 1:2) were fed in the dry reforming reaction to produce syngas while pure air was fed in the oxidation. A typical GSDR behavior is shown through the transient gas species composition and temperature over two cycles as depicted in Fig. 5 (larger number of cycles were completed demonstrating the stable repeatability of GSDR autothermal operation; only two are shown for illustration).

During the reduction stage, CO reacts with NiO to produce Ni and pure CO_2 stream ready for usage as feedstock in the reforming stage (otherwise it can be transported for storage in case of no-use). As can be seen in Fig. 5, almost complete conversion of CO (~99%) was achieved in the entire reduction period. It is worth mentioning that the reduction time was selected based on preliminary experiments showing that beyond 6 min a sharp drop in CO conversion occurs indicating depletion of oxygen on the oxygen carrier. Although this reduction reaction is slightly exothermic, the temperature slightly dropped across the stage due to substantial heat loss to the surrounding, but it remained beyond 800 °C before the start of the reforming stage. During this stage, CO_2 reacts with CH_4 producing syngas (CO and H_2). This reaction is catalyzed by the Ni sites of the oxygen carrier generated from the precedent reduction stage. Due to the high endothermic dry reforming reaction, the temperature drop at this stage intensifies, which is evident from the steepness of the temperature profile (Fig. 5). As the reforming proceeds, the reactor gets colder and CH_4 conversion drops leading to increased CH_4 slippage with an adverse effect on performance. It is, therefore, necessary to stop the reforming stage at a relatively high temperature to maintain high process performance. Alternatively, the GSDR cycle should be designed to start the reforming stage at a temperature higher than 850 °C to accommodate the inherent transient drop of temperature in the reforming stage. It is, however, worth mentioning that heat losses from the reactor contribute with the large extent in the sharp temperature drop that occurs in the reforming stage. Heat balance calculations of the present GSDR cycle plotted in Fig. 5 has shown that the achieved length of the reforming stage is only 50% of the theoretically predicted one. Indeed, for a total CO feed of ~2.6 mol to the reduction stage, ~6.15 mol of air would be required to oxidize back the oxygen carrier. The total heat generated in the system from the combustion of CO is then equal to ~700.9 kJ (assuming 95% CO conversion in the reduction stage). This heat is used for heating up the different feed gases from room temperature to the reactor operating temperature and the rest is utilized for driving the endothermic methane dry reforming reaction with an enthalpy of +247 kJ/mol. The calculated theoretical time of the reforming stage is ~543 s while the experimental one was only 280 s. Nevertheless, heat losses will be negligible in industrial scale reactor.

The GSDR cycle is finished by an oxidation stage by feeding air to oxidize back Ni to NiO with inherent separation of N_2 (depleted air) while serving as a main heat source for the GSDR cycle due to the highly exothermic oxidation reaction. This is clearly reflected on the temperature rise in the oxidation stage bringing it back to the initial target temperature for starting a new GSDR cycle. The oxygen carrier was completely oxidized back as reflected by the oxygen breakthrough from the gas composition plot (Fig. 5), where any longer air feed leads to heat removal from the system reducing. Therefore, to ensure optimal heat usage in the GSDR cycle, it is crucial to switch to the next reduction stage at the point where maximum oxidation temperature is attained which occurs just before oxygen breakthroughs in the oxidation stage.

3.2. The effect of temperature

The effect of temperature on the reactor performance at atmospheric pressure and CO_2/CH_4 molar ratio of 2 was investigated by varying the target start temperature from 750 °C – 850 °C. Equilibrium predictions were computed from HSC Chemistry using the assumptions and parameters similar to Snoeck et al (Xu and Froment, 1989; Snoeck et al., 2002, 1997) for comparison with the experimental results. An example of GSDR equilibrium composition at 1 bar, 800 °C and CO_2/CH_4 ratio of 2 is shown in Fig. 6. In addition, the equilibrium mole

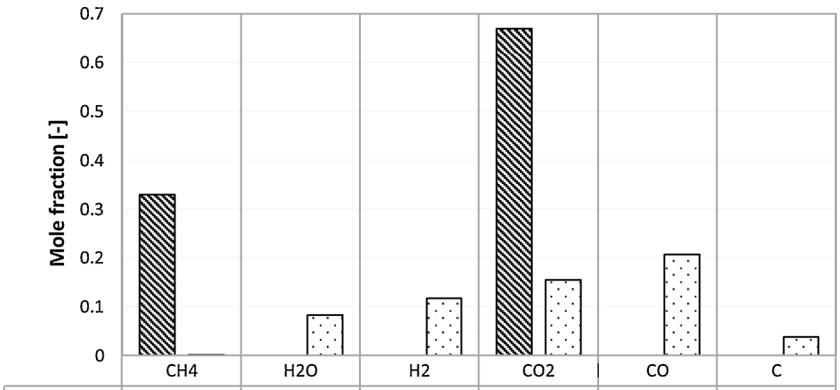

	CH4	H2O	H2	CO2	CO	C
Feed	0.33	0	0	0.67	0	0
Equilibrium	2.49299E-05	0.083152386	0.116807726	0.155141878	0.206593774	0.038259362

Fig. 6. Equilibrium dry reforming composition at 800 °C, 1 bar and CO_2/CH_4 molar ratio of 2.

fractions from 0 °C – 1000 °C at 1 bar, CO_2/CH_4 molar ratio of 2 and Ni/CH_4 molar ratio of 4 is shown in Fig. 7.

CO conversion in the reduction stage was sensitive to the operating temperature where the overall reduction stage CO conversion has moved from 86% at 750 °C to 98% at 850 °C (Fig. 8). The reforming stage was found to be more sensitive to temperature than the reduction stage. Fig. 9 shows the transient conversion of CH_4 and CO_2 across the reforming stage and the corresponding reactor temperature. It could be seen that for the three operating target temperatures that the reactor temperature drops gradually as the reforming stage proceeds. This arises from the heat losses and the high endothermicity of the reactions taking place in the reforming stage. Consequently, a very high difference in the CH_4 and CO_2 conversion is found between the start and the end of the reforming stage showing the large effect temperature has on the stage performance (Fig. 9). For example, methane conversion beyond 95% was achieved at the start of the reforming stage at a temperature of ~825 °C but dropped to 75% at the end of the stage where the reactor temperature reached ~700 °C (CO_2 conversion has shown a similar trend). This transient behavior of GSDR makes the overall reforming stage performance relatively low in comparison to what would be achieved with the interconnected fluidized bed reactor configuration where the fuel reactor where both oxygen carrier reduction and methane dry reforming occurs simultaneously under a steady state (Najera et al., 2011). However, integration of the GSDR concept with a GTL process as proposed in Section 1.1 could allow tolerating some unconverted methane in the reforming stage to feed directly to a GTL process. Then all the unconverted gases from GTL (a mixture of syngas, methane, CO_2, and steam) are to be recycled back to be converted in the reduction stage of GSDR, thereby maximizing fuel utilization and overall process efficiency. This potential of integration with a GLT process is not feasible with the interconnected fluidized bed reactor configuration unless a third reactor is added to complete a separate reduction and reforming stages, thus involving additional complexities to the process. Other alternatives to minimize the impact of the transient nature of the GSDR concept is the use of shorter reforming stage (shorter GSDR cycle), combined with operating the process at the higher target operating temperature, to complete the entire reforming stage at temperatures above 800 °C, in order to maximize fuel conversion. However, this will be compromised by lower CO_2 capture efficiency and purity that were shown earlier to be negatively affected when shortening the process cycle due to unavoidable mixing of gasses that occurs when switching between the stages (Zaabout et al., 2015b).

The large effect of temperature on the reforming stage performance could clearly be seen on the averaged conversion of CH_4 and CO_2 found to be well below equilibrium predictions at low operating temperature (especially for CH_4) but rapidly increases towards equilibrium at higher temperatures (see Figs. 7 and 10). This is consistent with thermodynamics since CH_4 and CO_2 are very stable molecules with high dissociation energy thus requires a high temperature to achieve equilibrium conversion (Jang et al., 2018). The transient nature of the GSDR process contributes to its low performance; with about 0.010$mol_{CH4}/g_{catalyst}$ is converted at 750 °C (average temperature of the reforming stage) which is slightly lower than the conversion 0.012$mol_{CH4}/g_{catalyst}$ achieved by Hao, et al. at 800 °C using a micro-fluidized bed reactor (Hao et al., 2009). The low conversion below equilibrium predictions at low temperatures could be attributed to the substantial carbon deposition that could result from competing mechanisms; Boudouard (***Reaction 4***) and methane cracking (***Reaction 3***) reactions (with the former being more favored at low temperature), driven by the well-known high catalytic activity of metallic nickel (the reduced Ni-based oxygen carrier) for carbon deposition (Muraza and Galadima, 2015a; Arora and Prasad, 2016; Wang et al., 1996). As shown in Fig. 12, beyond 700 °C carbon deposition becomes insignificant. This is because Boudouard reaction is not favoured at such high temperatures. This is in line with thermodynamics where the dry reforming reaction being more spontaneous and is favoured more than the methane cracking reaction leading to a decrease in carbon deposition. This is a promising result, showing that operation at industrially relevant temperatures (~1000 °C) will most likely not face noticeable carbon deposition problems, thereby GSDR contributes to solving one of the major issues affecting the commercialization of DMR (Jang et al., 2018; Arora and Prasad, 2016; Muraza and Galadima, 2015b). Carbon deposition also affects CO conversion at the reduction stage.

Although temperature plays a major role, it is difficult to generalize gas conversion by thermodynamics because it is also dependent on kinetics and the catalyst (Wei and Iglesia, 2004a, b; Wei and Iglesia, 2004c, d; Wei and Iglesia, 2004e, f; Usman et al., 2015b; Jang et al., 2018; Usman et al., 2015c). It is likely that due to kinetic limitation, the dry reforming reaction was slow at low temperature favoring the production of solid carbon on the catalyst and hydrogen from the converted methane. The synthesis method of the catalyst, active content, support and the number of active sites of catalyst also affect conversion and degree of reduction (Usman et al., 2015b; Jang et al., 2018). Too strong interaction of active metals and supports causes the poor reducibility and fuel conversion (Jang et al., 2018). Interestingly, despite the tens of GSDR cycles completed at different temperature that caused carbon deposition at different extents, no deactivation of the oxygen carrier/catalyst was observed demonstrating the robustness of the gas switching concept in prolonging the catalyst lifetime through cyclic gasification of the deposited carbon in the oxidation stage although on the expense of a reduced CO_2 capture and utilization efficiency. Note that the Ni-based oxygen carrier used in this study is a standard Ni/

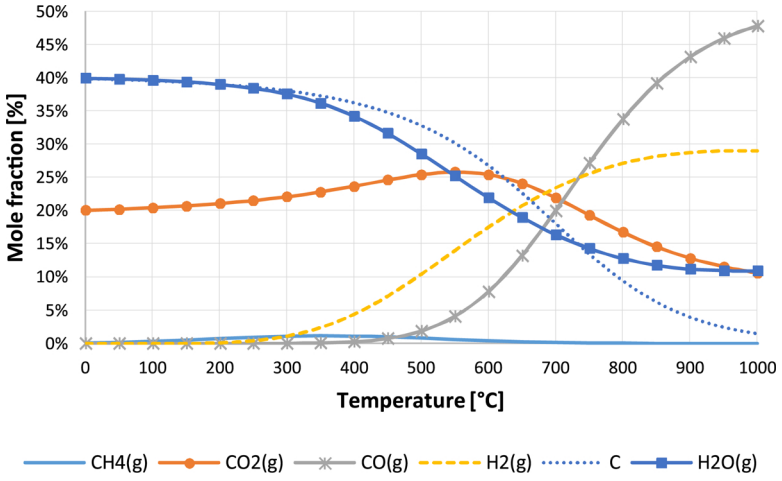

Fig. 7. Equilibrium gas composition of dry reforming composition from 0 to 1000 °C, at 1 bar, CO_2/CH_4 molar ratio of 2 and Ni/CH_4 molar ratio of 4.

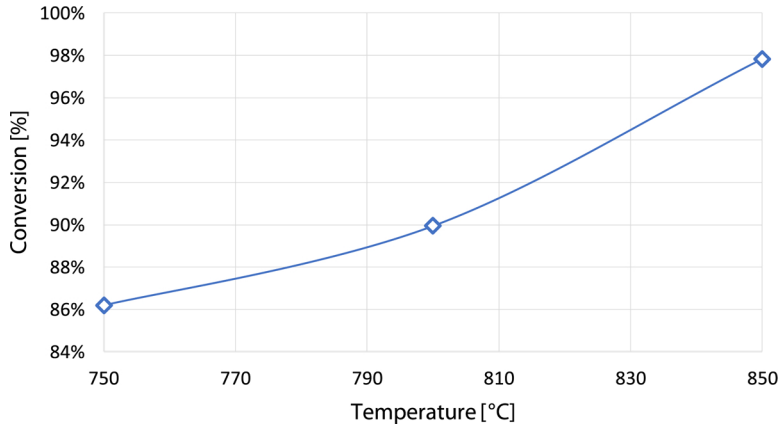

Fig. 8. Overall CO Conversion in the reduction stage plotted against the target operating temperature.

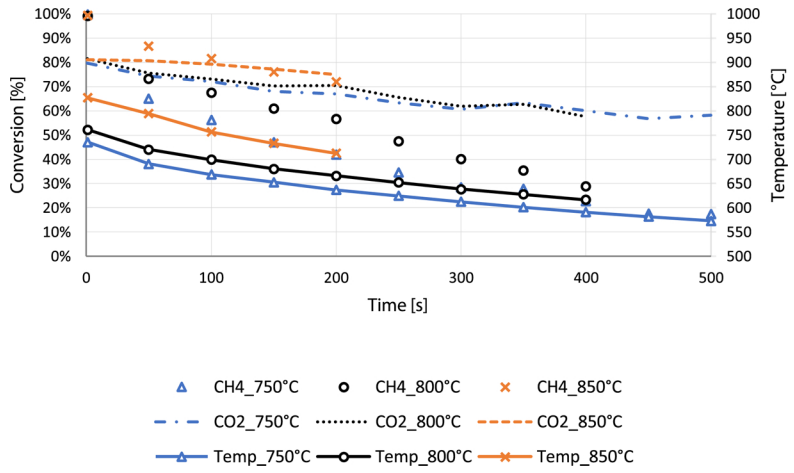

Fig. 9. Transient CH_4 and CO_2 conversion superposed with temperature profiles during the reforming stage for various target temperatures. 1 bar operating pressure, CO_2/CH_4 molar ratio of 2 and gas flowrate as follows: CO - 12.8 nl/min, CH_4 - 3.2 nl/min, CO_2 - 6.4 nl/min, Air −10 nl/min.

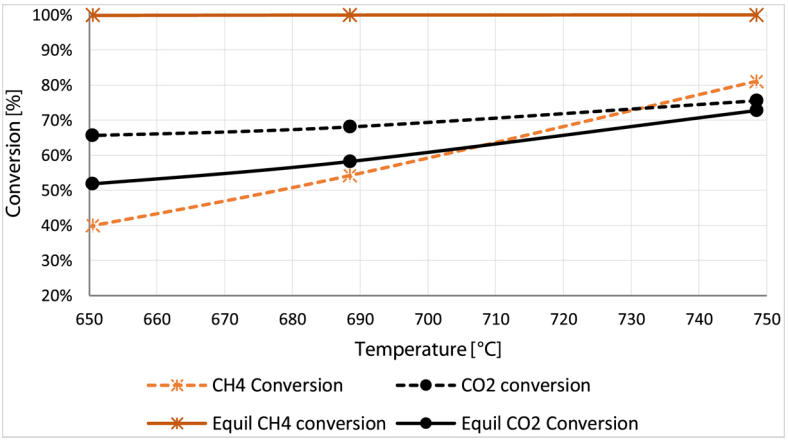

Fig. 10. Overall CH_4 and CO_2 conversion in the reforming stage plotted against the stage average temperature. 1 bar operating pressure, CO_2/CH_4 molar ratio of 2 and gas flowrate as follows: CO - 12.8 nl/min, CH_4 - 3.2 nl/min, CO_2 - 6.4 nl/min, Air −10 nl/min.

Al_2O_3 oxygen carrier that was tested under chemical looping combustion (Zaabout et al., 2013b), reforming (Wassie et al., 2017a, 2018; Osman et al., 2018) and no under dry reforming. Promoters would have been needed in the case of conventional DRM, without the redox reaction involved in the chemical looping, to reduce the extent of carbon deposition and extend the catalyst lifetime (e.g. K promoted support was used to improve the reducibility and reduce carbon deposition by creating weak interaction between the NiO/Ni and the support (Juan-Juan et al., 2006; Luna and Iriarte, 2008)).

Result also indicates low selectivity to H_2 as shown in Fig. 11. This could be explained by the RWGS (***Reaction 2***) that uses the excess of CO_2 feed and depletes the hydrogen produced from methane conversion to produce CO and H_2O, while the Boudouard reaction converts that CO back to more solid carbon. The continuous process combining the carbon deposition and RWSG mechanisms, explains the high conversion of CO_2 above the equilibrium prediction despite the low methane

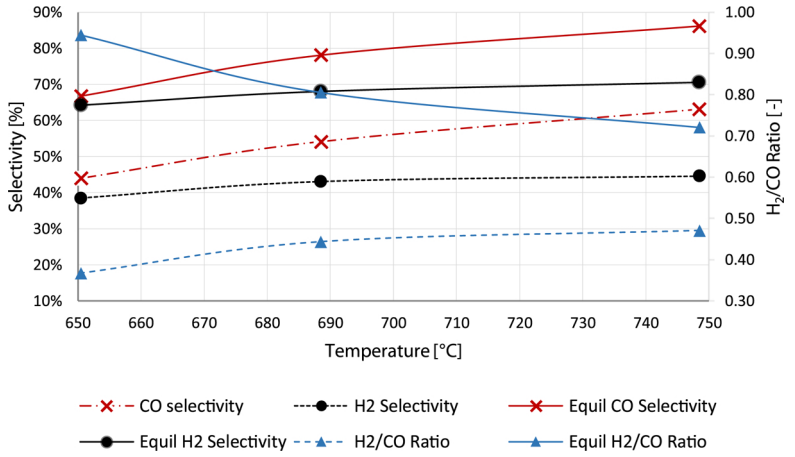

Fig. 11. Overall Selectivity and syngas ratio in the reforming stage plotted against the stage average temperature. 1 bar operating pressure, CO_2/CH_4 molar ratio of 2 and gas flowrate as follows: CO - 12.8 nl/min, CH_4 - 3.2 nl/min, CO_2 - 6.4 nl/min, Air −10 nl/min.

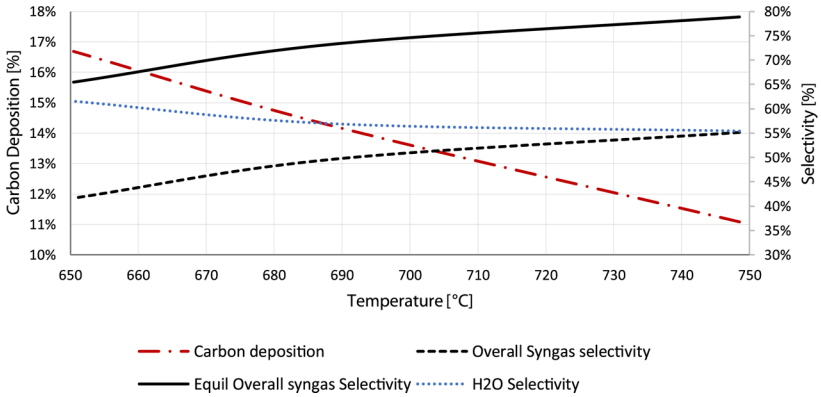

Fig. 12. Overall carbon deposition, steam selectivity and syngas selectivity in the reforming stage plotted against the stage average temperature. 1 bar operating pressure, CO_2/CH_4 molar ratio of 2 and gas flowrate as follows: CO - 12.8 nl/min, CH_4 - 3.2 nl/min, CO_2 - 6.4 nl/min, Air −10 nl/min.

conversion. This phenomenon has also favored carbon deposition rather than CO production with a CO selectivity way below equilibrium.

The change of Gibbs free energy can be used to determine which reaction route is favoured most at a particular temperature. The more the change in Gibbs energy tends towards negative the more favoured the reaction indicating that the free energy of the reactants is greater than that of the products, the entropy of the universe will increase in the reaction direction, thus the reaction will have more tendency to occur(Bejan, 2016). Consequently, the resulting overall syngas selectivity (Fig. 12) and H_2/CO ratio (Fig. 11) were relatively low similar to previous results of chemical looping dry reforming (Kang et al., 2018; Huang et al., 2016; Galvita et al., 2015). This conforms with thermodynamics as DMR is favoured more than RWGS at higher temperature considering the Gibbs-free energy value of, Table 1, resulting in lower CO yield similar to the previous experimental results of Khalesi et al. (Khalesi et al., 2008; Nikoo and Amin, 2011). The performance below the equilibrium prediction supports the previous results of Arora et al. stating that the DMR process is not only affected by thermodynamics but also kinetics (Arora and Prasad, 2016). If higher H_2/CO ratios are desired, reactant gas feed of lower C:H ratio should be maintained by reducing the CO_2/CH_4 ratio, co-feeding CO_2 with steam in tri-reforming or possible integration with WGS (Usman et al., 2015b; Jang et al., 2018; Pakhare and Spivey, 2014).

However, Fig. 12 also shows that the overall syngas selectivity increases with temperature. This could be attributed to the increase in gas conversion to syngas with reduced carbon formation. In general, higher temperatures will both minimize carbon deposition and maximize the syngas yield (CO and H_2). The GSDR process should, therefore, be operated at the highest achievable temperature.

3.3. The effect of CO_2/CH_4 ratio

Additional experiments were completed investigating the CO_2/CH_4 at 750 °C and 1 bar. Fig. 13 shows that CH_4 conversion increases with the CO_2/CH_4 ratio, which is in line with the findings of Arora and Prasad that CO_2 gas as an oxidant has a positive effect on CH_4

Table 1
Thermodynamic data of reactions 1-4: DMR, RWGS, Methane Cracking and Boudouard reactions respectively (source: HSC Chemistry).

T [°C]	ΔG [kJ]				ΔH [kJ]			
	Reaction 1	Reaction 2	Reaction 3	Reaction 4	Reaction 1	Reaction 2	Reaction 3	Reaction 4
750	−30.57	2.056	−21.715	8,854	259.478	34.633	89.078	−170,399
800	−44.741	0.477	−27.139	17,602	259.339	34.12	89.449	−169,890
850	−58.904	−1.079	−32.578	26,326	259.115	33.617	89.75	−169,365

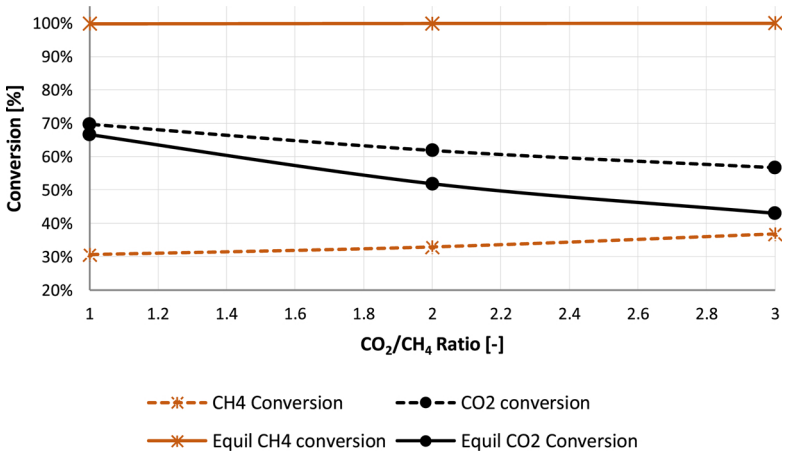

Fig. 13. Overall gas conversion in the reforming stage plotted against CO_2/CH_4 molar ratio. 1 bar operating pressure, 750 °C and gas flowrate as follows: CO - 12.8 nl/min, CH_4 - 3.2 nl/min, Air − 10 nl/min.

conversion (Arora and Prasad, 2016). The improvement in CH_4 conversion (Fig. 13) was however marginal with an excess of CO_2 at 750 °C, confirming the large effect that temperature has on overall reforming stage performance. Previous studies show that the initial step of dry reforming is methane decomposition (***Reaction 3***) to produce solid carbon and H_2 followed by the gasification of the solid C (***Reaction 15***) with CO_2 to produce CO (Usman et al., 2015b; Li et al., 2011). It could also be inferred from Fig. 15 that increasing CO_2/CH_4 has resulted in reduced carbon deposition. This agrees with the result of Nakagawa and Tomishige suggesting that the higher tendency towards carbon deposition will be observed in lower O/C (Li et al., 2011). As a matter of fact, carbon deposition arises mainly from CH_4 cracking and intensive CO_2 dissociation on the surface of the catalyst (Usman et al., 2015c). With insufficient reducible oxides (CO_2), the rate of methane decomposition will surpass CO_2 dissociation leading to carbon deposition (Usman et al., 2015b). It could also be speculated that the excess CO_2 has enhanced the RWGS (***Reaction 4***) that has consumed more H_2 for producing CO and H_2O (Fig. 15). These phenomena affect H_2/CO ratio as it decreases with the increase in CO_2/CH_4 ratio since a shift towards RWGS leads to more CO and less H_2 yield while a decrease in methane cracking as the partial pressure of CH_4 decrease also deteriorates H_2 yield (Figs. 14 and 15).

$$C + CO_2 \rightarrow 2CO \ (\Delta H_{298K} = +172.4 KJmol^{-1}) \quad (15)$$

3.4. The effect of oxygen carrier utilization

The oxygen carrier utilization was changed by varying the degree of reduction of the oxygen carrier before starting the reforming stage. In other words, 50% oxygen carrier utilization means that the oxygen carrier was 50% reduced (starting from a fully oxidized state), while 50% of the active content remains as NiO, before the start of the reforming stage. In this sensitivity study, 50% and 100% oxygen carrier utilizations were tested (the oxygen carrier is fully reduced to metallic nickel in the last case). 62% carbon deposition reduction in the case of 50% oxygen carrier utilization compared to 100% case (Fig. 17), reflecting the immediate positive impact of the presence of latent oxygen on the catalyst, in the form of NiO, during the reforming stage hindering carbon deposition likely through enabling oxy-gasification of the carbon. This has largely affected the mechanisms by which syngas is produced in the reforming stage. The oxy-gasification of carbon by latent oxygen on the catalyst favoured CO production that in turn reduced the extent of the RWGS reaction, leading to improved H_2 selectivity and consequently higher H_2/CO ratio and overall syngas selectivity. This also means that CO_2 conversion through the RWGS would reduce resulting in poorer overall CO_2 conversion in the reforming stage which was confirmed by the experimental results. Additionally, the 50% oxygen carrier utilization has also affected methane conversion that has shown a 22% reduction compared to the fully reduced catalyst (Fig. 16). The main reason for this could be the smaller availability of metallic Nickel sites to catalyze the dry reforming

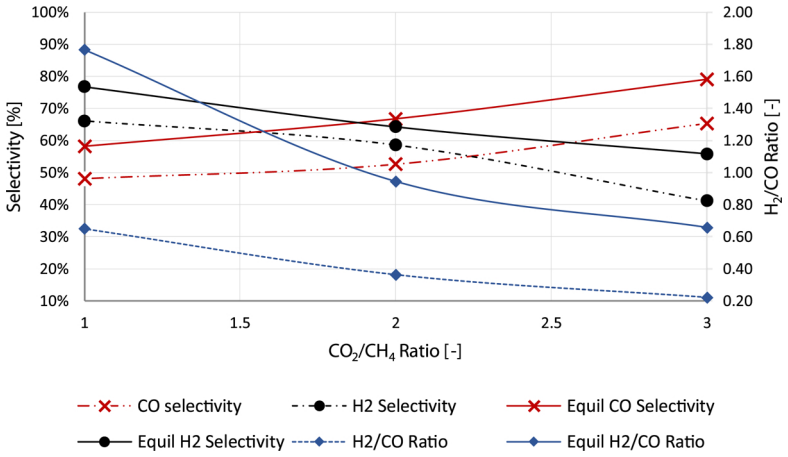

Fig. 14. Overall Selectivity and H_2/CO molar ratio in the reforming stage plotted against CO_2/CH_4 molar ratio. 1 bar operating pressure, 750 °C and gas flowrate as follows: CO - 12.8 nl/min, CH_4 - 3.2 nl/min, Air − 10 nl/min.

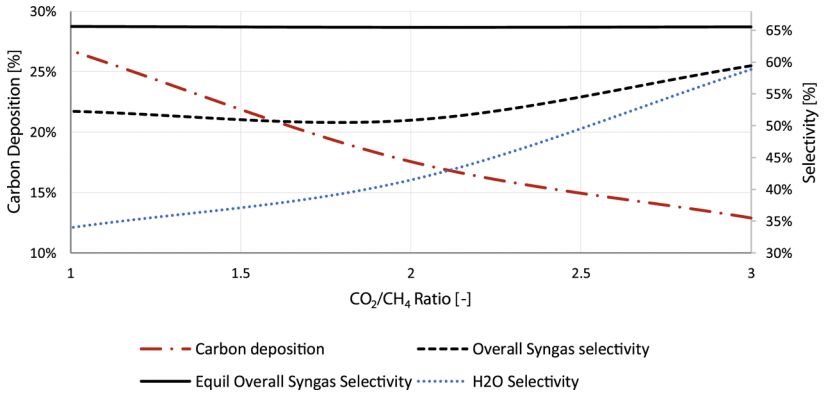

Fig. 15. Overall carbon deposition, steam selectivity and syngas selectivity in the reforming stage plotted against CO_2/CH_4 molar ratio. 1 bar operating pressure, 750 °C and gas flowrate as follows: CO- 12.8 nl/min, CH_4 - 3.2 nl/min, Air −10 nl/min.

reaction, as 50% of nickel on the oxygen carrier is present in oxidized form; NiO. This is in agreement with the finding from a previous study with the same oxygen carrier that has shown that steam methane reforming begins only when a good reduction level is reached on the oxygen carrier (Wassie et al., 2017b).

Another positive impact of smaller oxygen carrier utilization is the improved CO conversion in the reduction stage facilitated by the easily accessible latent oxygen in this case (Fig. 16). This further strengthens the business potential of integrating the GSDR with a GTL process, which will maximize the use of unconverted outlet stream gases from GTL in the reduction stage of GSDR. As mentioned in the introduction section, such integration with GTL will not be efficient if an interconnected fluidized configuration is used for the chemical looping dry reforming (Najera et al., 2011). In this case, the unconverted fuel gases in a GTL upstream will have to be fed jointly with methane to the fuel reactor of the interconnected fluidized bed configuration resulting in a methane-rich stream that leads to simultaneous oxygen carrier reduction and dry methane reforming reactions. This will have two negative impacts on the fuel reactor performance: i) lower fuel conversion will be achieved due to the low reactivity of methane with the oxidized oxygen carrier (Wassie et al., 2017b) and ii) the simultaneous DMR and reduction reactions will make it difficult to control the oxygen carrier utilization, thereby reducing the ability to achieve a high methane conversion, to control carbon deposition and to counteract the RWGS, and thus failing to solve the low H_2/CO ratio issue encountered in conventional dry reforming (Jang et al., 2018; Arora and Prasad, 2016; Muraza and Galadima, 2015b; Aramouni et al., 2018).

To summarize, the insights brought by the chemical looping process in general and particularly the gas switching to the dry reforming process, will largely reduce the issue raised in the introduction section that are hindering dry reforming commercialization: i) reduce CO_2 emissions from energy-intensive conventional dry reforming; instead using it as an added value chemical for the process ii) prolong the catalyst lifetime by gasifying the deposited carbon on the catalyst in the redox cycle and iii) solve the low H_2/CO ratio by partial oxygen carrier utilization. Clearly, the optimal operation of GSDR should consider tuning the three sensitivity parameters investigated in this section (temperature, CO_2/CH_4 ratio, and oxygen carrier utilization), in addition to considering the requirements of the downstream GTL process to integrate with GSDR. Further measures could be taken for approaching the H_2/CO ratio to unity such as using a proper oxygen carrier that both reduces carbon deposition and minimizes the extent of CO_2 and H_2 conversion through the RWGS. Co-feeding of steam would also minimize these issues, but it will reduce the extent of CO_2 use in GSDR (Zaabout et al., 2019). Alternatively, the GSDR system demonstrated in this work with the current oxygen carrier offers great opportunities for using renewable hydrogen from electrolysis to further improve CO_2 conversion in the reforming stage, but through the RWGS. Further research is needed both on the experimental and process integration aspects for better highlighting the full potential of GSDR in capturing and utilization of CO_2 for producing high-value chemicals and fuel at the highest possible efficiency.

4. Summary and conclusion

This paper extended the Gas Switching technology to dry methane

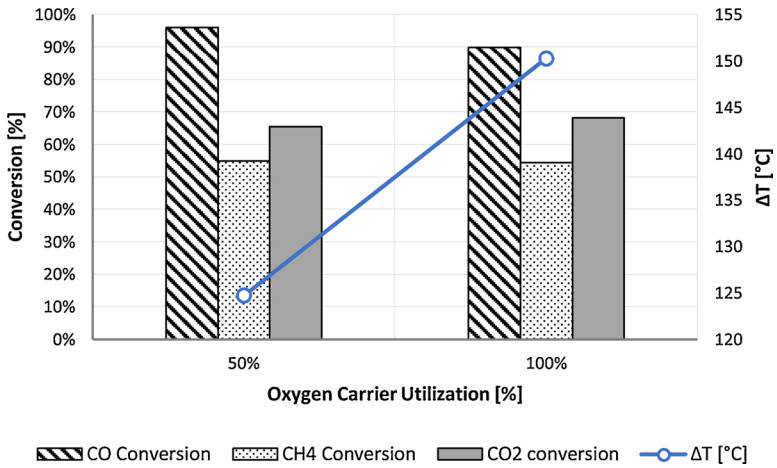

Fig. 16. Overall gas conversion and temperature change in the reforming stage plotted against Oxygen carrier utilization. 1 bar operating pressure, CO_2/CH_4 molar ratio of 2 and gas flowrate as follows: CO - 12.8 nl/min, CH_4 - 3.2 nl/min, CO_2 - 6.4 nl/min, Air −10 nl/min.

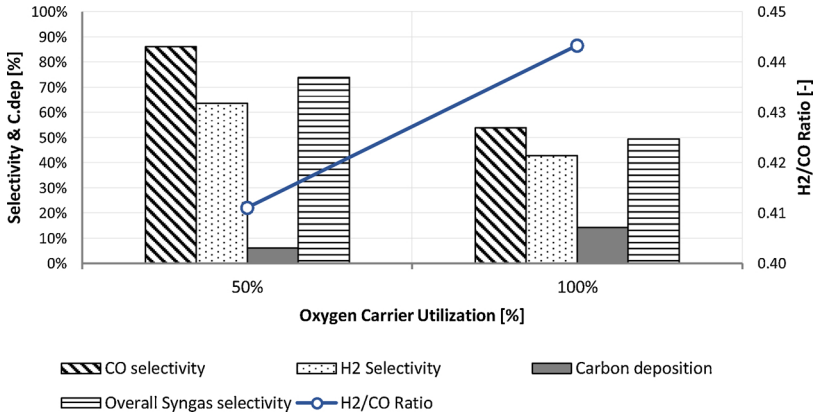

Fig. 17. Overall selectivity, carbon deposition and H_2/CO molar ratio in the reforming stage plotted against Oxygen carrier utilization. 1 bar operating pressure, CO_2/CH_4 molar ratio of 2 and gas flowrate as follows: CO - 12.8 nl/min, CH_4 - 3.2 nl/min, CO_2 - 6.4 nl/min, Air −10 nl/.

reforming, GSDR, for capturing and utilization of CO_2 in syngas production. This technology uses a single fluidized bed reactor cycling redox and reforming conditions into a bed of oxygen carrier, thereby greatly simplifying the operating and scale up challenges encountered in conventional chemical looping configuration.

Autothermal operation was experimentally demonstrated using the three-stages GSDR process (Reduction, Reforming and Oxidation) owing to the excellent heat integration between the different stages. The use of CO in the reduction stage was beneficial due to its slightly exothermic reaction with the Ni-based oxygen carrier allowing starting the reforming stage at a temperature high enough that ensured high CH_4 and CO_2 to syngas. However, the transient nature of the GSDR resulted in a continuous drop in temperature across the reforming stage causing a rapid deterioration of CH_4 and CO_2 conversions. In this respect, short GSDR cycle combined with elevated operation temperature would maximize GSDR performance in the reforming stage.

Carbon deposition was a major issue that results in reduced carbon capture efficiency, as the deposited carbon gasifies and combusts in the oxidation stage where the exhaust gases are vented to the atmosphere. Increasing the operating temperature and the CO_2/CH_4 proved to minimize carbon deposition, likely due to the overtake of the dry reforming reaction over methane cracking, but on the expenses of lower H_2/CO ratio of the produced syngas, driven by the reverse water gas shift reaction favored at higher temperature and excess of CO_2. Smaller oxygen carrier utilization (lower reduction degree) has also proved to reduce carbon deposition while increasing the H_2/CO ratio but caused lower CH_4 and CO_2 conversion. The remaining latent oxygen on the catalyst (when the oxygen carrier is 50% reduced) has likely reduced the catalytic activity of the three reactions taking place in the reforming stage (***Reaction 1***, ***Reaction 2*** and ***Reaction 3***). Additional benefits of smaller oxygen carrier utilization are the smaller temperature variation in the cycle that improves GSDR performance in the reforming stage and the better CO conversion in the reduction stage. It should also be emphasized that no deactivation was observed showing the robustness of the gas switching concept in prolonging the catalyst lifetime through cyclic gasification of the deposited carbon in the oxidation stage although on the expense of a reduced CO_2 capture and utilization efficiency.

Clearly, the key for GSDR performance optimization lays in the proper tuning of the process parameters investigated in this study, but also by using a more appropriate oxygen carrier/catalyst. Finally, integration of GSDR with a Gas-To-Liquid process (outlet stream from GSDR to GTL while unconverted hot gasses from GTL are to feed to the reduction stage of GSDR) has a great potential for maximizing fuel conversion and energy efficiency of the overall process.

Declaration of Competing Interest

The authors declare that they have no known competing financial interests or personal relationships that could have appeared to influence the work reported in this paper.

Acknowledgments

ACT GaSTech project. Project No 271511.

This project has received funding from The Research Council of Norway and is cofounded by the European Commission under the Horizon 2020 programme, ACT Grant Agreement No 691712. It also received the 2018 Equinor Publication Grant. VATL Lab technicians at the Norwegian University of Science and Technology are equally acknowledged for constructing and maintaining the experimental setup.

References

Anthony, E.J., 2008. Solid looping cycles: a new technology for coal conversion. Ind. Eng. Chem. Res. 47 (6), 1747–1754.
Aramouni, N.A.K., et al., 2017. Catalyst design for dry reforming of methane: analysis review. Renew. Sustain. Energy Rev.
Aramouni, N.A.K., et al., 2018. Catalyst design for dry reforming of methane: analysis review. Renew. Sustain. Energy Rev. 82, 2570–2585.
Arora, S., Prasad, R.J.R.A., 2016. An overview on dry reforming of methane: strategies to reduce carbonaceous deactivation of catalysts. RSC Adv. 6 (110), 108668–108688.
Baltagi, B.H., Bresson, G., Pirotte, A., 2002. Comparison of forecast performance for homogeneous, heterogeneous and shrinkage estimators: some empirical evidence from US electricity and natural-gas consumption. Econ. Lett. 76 (3), 375–382.
Bejan, A., 2016. Advanced Engineering Thermodynamics. John Wiley & Sons.
Bolhar-Nordenkampf, J., et al., 2009. Performance of a NiO-based oxygen carrier for chemical looping combustion and reforming in a 120kW unit. In: Gale, J., Herzog, H., Braitsch, J. (Eds.), Greenhouse Gas Control Technologies 9, pp. 19–25.
Carrara, C., et al., 2008. Kinetic and stability studies of Ru/La 2 O 3 used in the dry reforming of methane. Top. Catal. 51 (1-4), 98–106.
Chen, P., et al., 1998. Development of coking-resistant Ni-based catalyst for partial oxidation and CO2-reforming of methane to syngas. Appl. Catal. A Gen. 166 (2), 343–350.
Cho, P., Mattisson, T., Lyngfelt, A., 2004. Comparison of iron-, nickel-, copper- and manganese-based oxygen carriers for chemical-looping combustion. Fuel 83 (9), 1215–1225.
de Diego, L.F., et al., 2009. Hydrogen production by chemical-looping reforming in a circulating fluidized bed reactor using Ni-based oxygen carriers. J. Power Sources 192 (1), 27–34.
Ding, N., et al., 2012. Development and testing of an interconnected fluidized-bed system for chemical looping combustion. Chem. Eng. Technol. 35 (3), 532–538.
Ewbank, J.L., et al., 2014. Effect of preparation methods on the performance of Co/Al 2 O 3 catalysts for dry reforming of methane. Green Chem. 16 (2), 885–896.
Galvita, V.V., et al., 2015. Catalyst-assisted chemical looping for CO2 conversion to CO. Appl. Catal. B 164, 184–191.
Hamers, H.P., et al., 2014. Comparison on process efficiency for CLC of syngas operated in

packed bed and fluidized bed reactors. Int. J. Greenh. Gas Control. 28 (0), 65–78.
Hamers, H.P., et al., 2013. A novel reactor configuration for packed bed chemical-looping combustion of syngas. Int. J. Greenh. Gas Control. 16 (0), 1–12.
Hao, Z., et al., 2009. Characterization of aerogel Ni/Al2O3 catalysts and investigation on their stability for CH4-CO2 reforming in a fluidized bed. Fuel Process. Technol. 90 (1), 113–121.
Hou, Z., et al., 2006. Production of synthesis gas via methane reforming with CO2 on noble metals and small amount of noble-(Rh-) promoted Ni catalysts. Int. J. Hydrogen Energy 31 (5), 555–561.
Huang, Z., et al., 2016. Evaluation of multi-cycle performance of chemical looping dry reforming using CO2 as an oxidant with Fe–Ni bimetallic oxides. J. Energy Chem. 25 (1), 62–70.
IPCC, 2018. Global Warming of 1.5C- An IPCC Special Report on the Impacts of Global Warming of 1.5C Above Pre-industrial Levels and Related Global Greenhouse Gas Emission Pathways, in the Context of Strengthening the Global Response to the Threat of Climate Change, Sustainable Development, and Efforts to Eradicate Poverty. Summary for Policymakers. IPCC, Switzerland.
Ishida, M., Zheng, D., Akehata, T., 1987. Evaluation of a chemical-looping-combustion power-generation system by graphic exergy analysis. Energy 12 (2), 147–154.
Jang, W.-J., et al., 2018. A review on dry reforming of methane in aspect of catalytic properties. Catal. Today.
Johansson, E., et al., 2006. A 300 W laboratory reactor system for chemical-looping combustion with particle circulation. Fuel 85 (10–11), 1428–1438.
Juan-Juan, J., Román-Martínez, M., Illán-Gómez, M., 2006. Effect of potassium content in the activity of K-promoted Ni/Al2O3 catalysts for the dry reforming of methane. Appl. Catal. A Gen. 301 (1), 9–15.
Kang, D., et al., 2018. Syngas production on a Ni-enhanced Fe2O3/Al2O3 oxygen carrier via chemical looping partial oxidation with dry reforming of methane. Appl. Energy 211, 174–186.
Khalesi, A., Arandiyan, H.R., Parvari, M., 2008. Effects of lanthanum substitution by strontium and calcium in La-Ni-Al perovskite oxides in dry reforming of methane. Chinese J. Catal. 29 (10), 960–968.
Kolbitsch, P., et al., 2010. Operating experience with chemical looping combustion in a 120 kW dual circulating fluidized bed (DCFB) unit. Int. J. Greenh. Gas Control. 4 (2), 180–185.
Kronberger, B., et al., 2004. A two-compartment fluidized bed reactor for CO2 capture by chemical-looping combustion. Chem. Eng. Technol. 27 (12), 1318–1326.
Li, D., Nakagawa, Y., Tomishige, K., 2011. Methane reforming to synthesis gas over Ni catalysts modified with noble metals. Appl. Catal. A Gen. 408 (1–2), 1–24.
Linderholm, C., et al., 2008. 160 h of chemical-looping combustion in a 10 kW reactor system with a NiO-based oxygen carrier. Int. J. Greenh. Gas Control. 2 (4), 520–530.
Luna, A.E.C., Iriarte, M.E., 2008. Carbon dioxide reforming of methane over a metal modified Ni-Al2O3 catalyst. Appl. Catal. A Gen. 343 (1-2), 10–15.
Lyngfelt, A., Leckner, B., Mattisson, T., 2001. A fluidized-bed combustion process with inherent CO2 separation; application of chemical-looping combustion. Chem. Eng. Sci. 56 (10), 3101–3113.
Muraza, O., Galadima, A., 2015a. A review on coke management during dry reforming of methane. Int. J. Energy Res. 39 (9), 1196–1216.
Muraza, O., Galadima, A., 2015b. A review on coke management during dry reforming of methane. Int. J. Energy Res. 39 (9), 1196–1216.
Najera, M., et al., 2011. Carbon capture and utilization via chemical looping dry reforming. Chem. Eng. Res. Des. 89 (9), 1533–1543.
Nazir, S.M., et al., 2018. Techno-economic assessment of the novel gas switching reforming (GSR) concept for gas-fired power production with integrated CO2 capture. Int. J. Hydrogen Energy 43 (18), 8754–8769.
Nejat, P., et al., 2015. A global review of energy consumption, CO2 emissions and policy in the residential sector (with an overview of the top ten CO2 emitting countries). Renew. Sustain. Energy Rev. 43, 843–862.
Nikoo, M.K., Amin, N., 2011. Thermodynamic analysis of carbon dioxide reforming of methane in view of solid carbon formation. Fuel Process. Technol. 92 (3), 678–691.
Noorman, S., van Sint Annaland, M., Kuipers, 2007. Packed bed reactor technology for chemical-looping combustion. Ind. Eng. Chem. Res. 46 (12), 4212–4220.
Ortiz, M., et al., 2011. Optimization of hydrogen production by chemical-looping autothermal reforming working with Ni-based oxygen-carriers. Int. J. Hydrogen Energy 36 (16), 9663–9672.
Osman, M., et al., 2018. Internally circulating fluidized-bed reactor for syngas production using chemical looping reforming. Chem. Eng. J.
Oyama, S.T., et al., 2012. Dry reforming of methane has no future for hydrogen production: comparison with steam reforming at high pressure in standard and membrane reactors. Int. J. Hydrogen Energy 37 (13), 10444–10450.
Pakhare, D., Spivey, J., 2014. A review of dry (CO 2) reforming of methane over noble metal catalysts. Chem. Soc. Rev. 43 (22), 7813–7837.
Proell, T., et al., 2010. Syngas and a separate nitrogen/argon stream via chemical looping reforming - A 140 kW pilot plant study. Fuel 89 (6), 1249–1256.
Rydén, M., Arjmand, M., 2012. Continuous hydrogen production via the steam–iron reaction by chemical looping in a circulating fluidized-bed reactor. Int. J. Hydrogen Energy 37 (6), 4843–4854.
Ryden, M., Lyngfelt, A., 2006. Using steam reforming to produce hydrogen with carbon dioxide capture by chemical-looping combustion. Int. J. Hydrogen Energy 31 (10), 1271–1283.
Rydén, M., Lyngfelt, A., Mattisson, T., 2006. Synthesis gas generation by chemical-looping reforming in a continuously operating laboratory reactor. Fuel 85 (12–13), 1631–1641.
Snoeck, J.-W., Froment, G., Fowles, M., 2002. Steam/CO2 reforming of methane. Carbon filament formation by the Boudouard reaction and gasification by CO2, by H2, and by steam: kinetic study. Ind. Eng. Chem. Res. 41 (17), 4252–4265.
Snoeck, J.-W., Froment, G., Fowles, M., 1997. Kinetic study of the carbon filament formation by methane cracking on a nickel catalyst. J. Catal. 169 (1), 250–262.
Sternberg, A., Jens, C.M., Bardow, A.J.G.C., 2017. Life cycle assessment of CO 2-based C1-chemicals. Green Chem. 19 (9), 2244–2259.
Ugwu, A., et al., 2019. Gas Switching reforming for syngas production with iron-based oxygen carrier-the performance under pressurized conditions. Int. J. Hydrogen Energy.
Usman, M., Daud, W.W., Abbas, H.F., 2015a. Dry reforming of methane: influence of process parameters—a review. Renew. Sustain. Energy Rev. 45, 710–744.
Usman, M., Daud, W.W., Abbas, H.F., 2015b. Dry reforming of methane: influence of process parameters—a review. Renew. Sustain. Energy Rev. 45, 710–744.
Usman, M., et al., 2015c. Dry reforming of methane: influence of process parameters—a review. Renew. Sustain. Energy Rev. 45, 710–744.
Wang, S., et al., 1996. Carbon dioxide reforming of methane to produce synthesis gas over metal-supported catalysts: state of the art. Energy Fuels 10 (4), 896–904.
Wassie, S.A., et al., 2018. Hydrogen production with integrated CO2 capture in a membrane assisted gas switching reforming reactor: proof-of-Concept. Int. J. Hydrogen Energy 43 (12), 6177–6190.
Wassie, S.A., et al., 2017a. Hydrogen production with integrated CO2 capture in a novel gas switching reforming reactor: proof-of-concept. Int. J. Hydrogen Energy 42 (21), 14367–14379.
Wassie, S.A., et al., 2017b. Hydrogen production with integrated CO2 capture in a novel gas switching reforming reactor: proof-of-concept. Int. J. Hydrogen Energy 42 (21), 14367–14379.
Wei, J., Iglesia, E., 2004a. Isotopic and kinetic assessment of the mechanism of reactions of CH4 with CO2 or H2O to form synthesis gas and carbon on nickel catalysts. J. Catal. 224 (2), 370–383.
Wei, J., Iglesia, E., 2004b. Structural and mechanistic requirements for methane activation and chemical conversion on supported iridium clusters. Angew. Chem. Int. Ed. 43 (28), 3685–3688.
Wei, J., Iglesia, E., 2004c. Mechanism and site requirements for activation and chemical conversion of methane on supported Pt clusters and turnover rate comparisons among noble metals. J. Phys. Chem. B 108 (13), 4094–4103.
Wei, J., Iglesia, E., 2004d. Isotopic and kinetic assessment of the mechanism of methane reforming and decomposition reactions on supported iridium catalysts. Angew. Chem. Int. Ed. 6 (13), 3754–3759.
Wei, J., Iglesia, E., 2004e. Structural requirements and reaction pathways in methane activation and chemical conversion catalyzed by rhodium. J. Catal. 225 (1), 116–127.
Wei, J., Iglesia, E., 2004f. Reaction pathways and site requirements for the activation and chemical conversion of methane on Ru− based catalysts. J. Phys. Chem. B 108 (22), 7253–7262.
Xu, J., Froment, G.F., 1989. Methane steam reforming, methanation and water-gas shift: I. Intrinsic kinetics. Aiche J. 35 (1), 88–96.
Zaabout, A., Cloete, S., Amini, S., 2014. Hydrodynamic investigation into a novel IC-CLC reactor concept for power production with integrated CO2 capture. 10th International Conference on Computational Fluid Dynamics in the Oil & Gas, Metallurgical and Process Industries.
Zaabout, A., Cloete, S., Amini, S., 2017. Autothermal operation of a pressurized Gas Switching Combustion with ilmenite ore. Int. J. Greenh. Gas Control. 63, 175–183.
Zaabout, A., et al., 2018. A pressurized Gas Switching Combustion reactor: Autothermal operation with a CaMnO3−δ-based oxygen carrier. Chem. Eng. Res. Des. 137, 20–32.
Zaabout, A., et al., 2019. Gas Switching reforming (GSR) for syngas production with integrated CO2 capture using iron-based oxygen carriers. Int. J. Greenh. Gas Control. 81, 170–180.
Zaabout, A., et al., 2013a. Experimental demonstration of a novel gas switching combustion reactor for power production with integrated CO2 capture. Ind. Eng. Chem. Res. 52 (39), 14241–14250.
Zaabout, A., et al., 2015a. A novel gas switching combustion reactor for power production with integrated CO2 capture: sensitivity to the fuel and oxygen carrier types. Int. J. Greenh. Gas Control. 39, 185–193.
Zaabout, A., et al., 2013b. Experimental demonstration of a novel gas switching combustion reactor for power production with integrated CO2 capture. Ind. Eng. Chem. Res. 52 (39), 14241–14250.
Zaabout, A., et al., 2015b. A novel gas switching combustion reactor for power production with integrated CO2 capture: sensitivity to the fuel and oxygen carrier types. Int. J. Greenhouse Gas Control 39, 185–193.